TESTING THE IMPACT-INDUCED DECOMPRESSION MELTING HYPOTHESIS FOR ROCKY, MAFIC INFILLED CRATER FLOORS ON MARS. C. S. Edwards[1], P. D. Asimow[1], B. L. Ehlmann[1], S. Stewart-Mukhopadhyay[2]; [1]California Institute of Technology, Division of Geological and Planetary Sciences, cedwards@caltech.edu; [2]Harvard University, Department of Earth and Planetary Sciences.

Introduction:

Deeply infilled craters were first observed by Mariner 4 in 1965 and have remained an enigma ever since. Various processes to fill martian craters have been proposed, including aeolian sedimentation [e.g. 1, 2, 3], lacustrine sedimentation [e.g. 4, 5] and impact processes such as impact melt ponding [e.g. 6, 7, 8]. However, these explanations cannot explain all occurrences of infilled craters [9].

Mapping of high-thermal inertia surfaces, defined as >1200 J K^{-1} m^{-2} $s^{-1/2}$ and interpreted as exposed bedrock, was conducted globally on Mars between 75˚S and 75˚N [10] using Thermal Emission Imaging System (THEMIS) nighttime infrared data. Edwards et al. [9] conducted a globally comprehensive compositional, thermophysical and morphological study of ~2800 flat floored, high thermal inertia craters (Fig.1), where bedrock is exposed in the floor directly adjacent to the lower thermal inertia crater walls (Figs. 1 & 2). Edwards et al [9] characterized the geologic setting of these crater floors using a variety of compositional (Thermal Emission Spectrometer, TES; Thermal Emission Imaging System, THEMIS; Compact Reconnaissance Imaging Spectrometer for Mars; CRISM), thermophysical (THEMIS), and morphological datasets (High Resolution Imaging Science Experiment, HiRISE; Context Imager, CTX) along with crater size frequency model ages from over 110 crater floors (resulting in formation ages of ~3.5-4Ga). The geologic characteristics of these crater floor deposits (rocky, enriched in olivine/pyroxene, lobate margins and wrinkle ridges) resulted in an interpretation that the infilling material was likely volcanic in origin. However, the source for the infilling material is enigmatic, as no vents are observed and these deposits do not occur in association with any specific volcanic or geographic provinces. Edwards et al., [9] proposed that a different process – impact excavation-induced decompression melting of the martian mantle – is responsible for the intra-crater materials.

In this work, we present the quantitative modeling of this process through two different techniques: 1) coupling of the MELTS [11, 12] thermodynamic model for silicate magmas to a shock physics CTH impact model with realistic rock rheology [13, 14] and 2) a more petrological treatment following [15] where *in situ* decompression melting (occurring immediately following excavation) and adiabatic melting as the lithosphere becomes isostatically supported (over longer timescales) can be estimated.

Model Inputs:

The initial conditions for each model are established from the literature for early and modern Mars mantle potential temperatures [16], paleo- to modern-surface heat flux estimates [16-20] and an estimate of radiogenic crustal heat production ($1.7x10^{-10}$ and $5.0x10^{-11}$ W/kg for 4 Ga and modern Mars respectively). These parameters were used in combination with the density and thermal conductivity of basalt (2.89

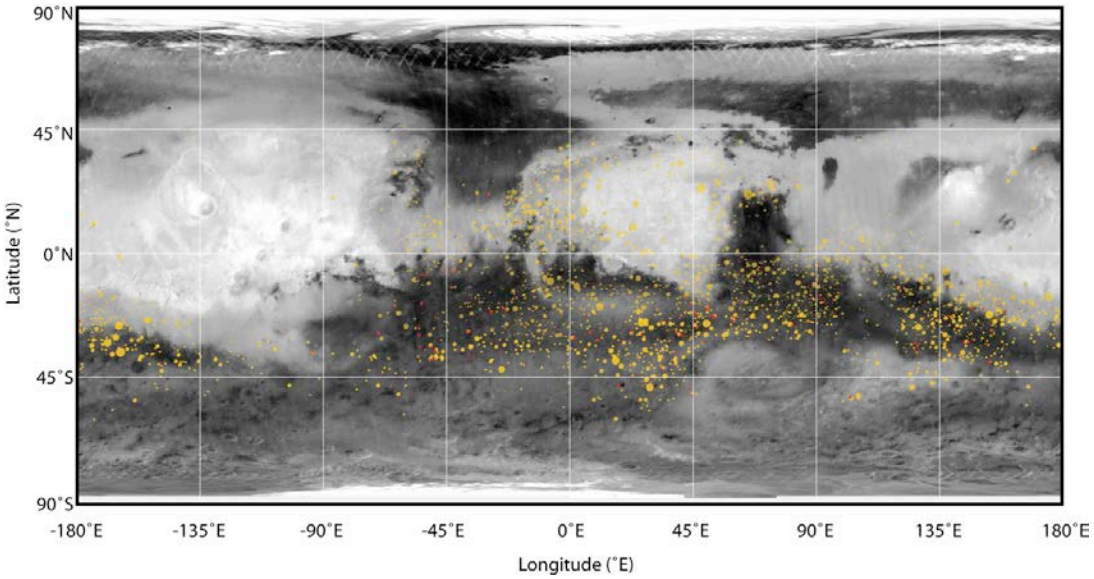

Fig. 1. *Global distribution of high thermal inertia, flat-floored craters that are commonly enriched in pyroxene and olivine relative to plagioclase and high-Si phases compared to typical surrounding highlands material. Red=[10]; Yellow=[9]*

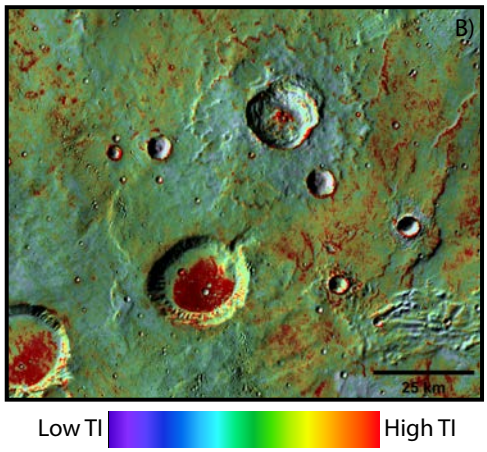

Fig. 2: *Example high thermal inertia, flat crater floor [9]*

J/m/K/s, 2950 kg/m^3) and perdiotite (3.5 J/m/K/s, 3500 kg/m^3) to calculate a variety of geotherms for Mars with a stagnant conductive lid with radiogenic heat production for the crustal component (Figure 3, Table 1). The mantle temperature profile was calculated using MELTS with a Dreibus and Wanke [22] mantle composition. Lithospheric thickness is determined by the intercept of the lithosphere and mantle geotherms.

Outcomes and Expected Significance:

The exact conditions under which impact-induced decompression melting occurs, if at all [23], are not well-constrained. Some models [15] have found that instantaneous decompression melting is possible under the right conditions for large impacts, though relatively small variations in impactor diameter, lithospheric thickness, and mantle potential temperature can have a significant impact on decompression melt volume production (e.g., a 50 ˚C increase in mantle potential temperature results in an increase in melt volume by a factor of 2 or 3 [15]). Furthermore, the early (ca. 4 Ga) thermal gradients and lithospheric conditions present on rocky bodies are poorly constrained, though this early time in planetary evolution likely coincided with a thin lithosphere and high mantle potential temperature, making it most conducive for widespread impact-induced decompression melting.

We offer a multi-faceted approach to this problem understanding that the most modern numerical impact models may not fully encompass all the dynamical processes that occur in an impact. By using a simplified, primarily petrologic treatment of the problem combined with the sophisticated impact model, we aim to place constraints on the thermal and lithospheric conditions that could give rise to impact-induced decompression. Strong evidence exists in the Martian geologic record that craters were infilled with olivine/pyroxene-rich volcanic material early in its history but not later [9]. These observations, when coupled with the numerical models presented here, have the potential to constrain early planetary evolutionary models.

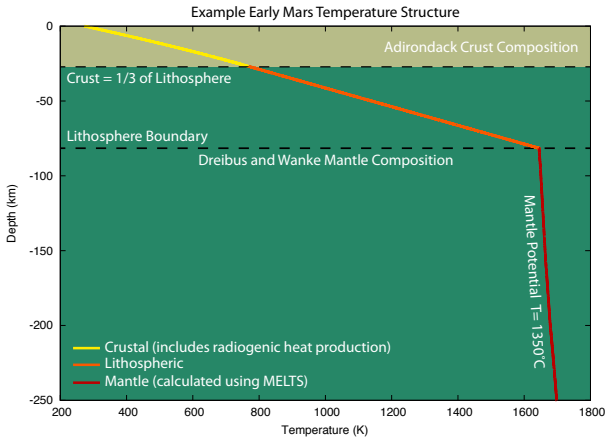

Fig. 3: *Example thermal profile for early Mars conditions, with a surface heat flux of 60 mW/m^2, a mantle potential temperature of 1350˚C, a paleo crustal heat production value of 5.0x10^{-11} W/kg and the crustal/mantle compositions and thermophysical properties described above.*

Table 1: parameter ranges under consideration

Crater Diameter (km)	Surface Heat Flux (mW/m^2)	Mantle Potential Temperature (˚C)
20	20	1250
50	40	1350
80	60	1450
110	80	1550

References:

[1] P. R. Christensen, (1983) *Icarus* **56**, 496. [2] R. E. Arvidson, (1974) *Icarus* **21**, 12. [3] M. L. McDowell, V. E. Hamilton, (2007) *J. Geophys. Res.* **112**, E12001. [4] M. Pondrelli *et al.*, (2005) *J. Geophys. Res.* **110**. [5] N. A. Cabrol, E. A. Grin, (1999) *Icarus* **142**, 160. [6] P. H. Schultz, (1976) *The Moon* **15**, 241. [7] S. Smrekar, C. M. Pieters, (1985) *Icarus* **63**, 442. [8] D. E. Wilhelms *et al.*, (1987). [9] C. S. Edwards *et al.*, (2014) *Icarus* **228**, 149. [10] C. S. Edwards *et al.*, (2009) *J. Geophys. Res* **114**, E11001. [11] M. S. Ghiorso *et al.*, (2002) *Geochemistry Geophysics Geosystems* **3**, 1030. [12] P. M. Smith, P. D. Asimow, (2005) *Geochemistry, Geophysics, Geosystems* **6**, Q02004. [13] L. E. Senft, S. T. Stewart, (2007) *J. Geophys. Res: Planets* **112**, E11002. [14] L. E. Senft, S. T. Stewart, (10/15/, 2009) *Earth Planet Sc Lett* **287**, 471. [15] L. T. Elkins-Tanton, B. H. Hager, (2005) *Earth Planet Sc Lett* **239**, 219. [16] A. Morschhauser *et al.*, (2011) *Icarus* **212**, 541. [17] E. M. Parmentier, M. T. Zuber, (2007) *J. Geophys Res.* **112**. [18] D. Baratoux *et al.*, (2011) *Nature* **472**, 338. [19] M. Grott, D. Breuer, (Jun, 2009) *Icarus* **201**, 540. [20] P. J. McGovern *et al.*, (2002) *J. Geophys. Res* **107**. [21] B. C. Hahn *et al.*, (Jul, 2011) *Geophys Res Lett* **38**. [22] G. Dreibus, H. Wanke, (1985) *Meteoritics* **20**, 367. [23] B. Ivanov, H. Melosh, (2003) *Geology* **31**, 869.